Pharmacokinetic and Metabolomic Studies with BBT-059 in Nonhuman Primates Exposed to Total-Body Gamma Radiation

Authors: Carpenter, Alana D., Li, Yaoxiang, Miranda, Issa Melendez, Wise, Stephen Y., Fatanmi, Oluseyi O., et al.

Source: Radiation Research, 203(2) : 83-95

Published By: Radiation Research Society

URL: https://doi.org/10.1667/RADE-24-00219.1

RADIATION RESEARCH **203**, 83–95 (2025)
0033-7587/25 $15.00

DOI: 10.1667/RADE-24-00219.1

Pharmacokinetic and Metabolomic Studies with BBT-059 in Nonhuman Primates Exposed to Total-Body Gamma Radiation

Alana D. Carpenter,[a,b] Yaoxiang Li,[c] Issa Melendez Miranda,[a,b] Stephen Y. Wise,[a,b] Oluseyi O. Fatanmi,[a,b] Sarah A. Petrus,[a,b] Christine M. Fam,[d] Sharon J. Carlson,[d] George N. Cox,[d] Amrita K. Cheema,[c,e] Vijay K. Singh[a,b,1]

[a] Division of Radioprotectants, Department of Pharmacology and Molecular Therapeutics, F. Edward Hébert School of Medicine, Uniformed Services University of the Health Sciences, Bethesda, Maryland; [b] Armed Forces Radiobiology Research Institute, Uniformed Services University of the Health Sciences, Bethesda, Maryland; [c] Department of Oncology, Lombardi Comprehensive Cancer Center, Georgetown University Medical Center, Washington, D.C.; [d] Bolder BioTechnology, Boulder, Colorado; [e] Department of Biochemistry, Molecular and Cellular Biology, Georgetown University Medical Center, Washington, D.C.

Carpenter AD, Li Y, Miranda IM, Wise SY, Fatanmi OO, Petrus SA, Fam CM, Carlson SJ, Cox GN, Cheema AK, Singh VK. Pharmacokinetic and Metabolomic Studies with BBT-059 in Nonhuman Primates Exposed to Total-body Gamma Radiation. Radiat Res. 203, 83–95 (2025).

BBT-059 is a long-acting PEGylated interleukin-11 analog that has been shown to have hematopoiesis-promoting and anti-apoptotic attributes, and is being studied as a radiation countermeasure for the hematopoietic acute radiation syndrome (H-ARS). This potential countermeasure has been demonstrated to enhance survival in irradiated mice. To investigate the toxicity and safety profile of this agent, 14 nonhuman primates (NHPs, rhesus macaques) were administered two different doses of BBT-059 subcutaneously 24 h after 4 Gy total-body irradiation and were monitored for the next 60 days postirradiation. Blood samples were investigated for the pharmacokinetics and pharmacodynamics of this agent and its effects on complete blood counts, cytokines, vital signs, and metabolomics. No adverse health effects were observed in either treatment group. Radiation-induced metabolomic dysregulation was observed in both treatment groups, and BBT-059 afforded some short-term radiomitigation. A few pathways were commonly dysregulated by radiation exposure including steroid hormone biosynthesis pathways, fatty acid activation, and glycerophospholipid metabolism. Notably, radiation-induced dysregulation to the linoleate metabolism pathway was significantly mitigated by either dose of BBT-059. In brief, this study suggests that BBT-059 has a good safety profile in irradiated NHPs and that its development as a medical countermeasure for U.S. Food and Drug Administration approval for human use should be continued.

INTRODUCTION

Increasing risks of radiological and nuclear accidents and terrorism continue to challenge national capabilities to maintain global non-proliferation and security (*1*). This has renewed interest in developing radiation medical countermeasures (MCMs) for clinically significant ionizing radiation exposure. The availability of non-toxic, safe, and efficacious MCMs against these threats represents an important unmet medical need. To expedite the development of MCMs, the United States Food and Drug Administration (U.S. FDA) has implemented the Animal Rule that applies to the development and testing of new MCMs to reduce or prevent life-threatening conditions caused by exposure to lethal or disabling chemical, biological, radiological, and nuclear agents when human efficacy trials are not possible (*2*, *3*).

Ionizing radiation exposures can result in different types of injuries requiring diagnostic and therapeutic measures. The clinical progression and outcome of the acute radiation syndrome (ARS) depends on the absorbed radiation dose (*4*). Clinical manifestations of ARS in humans include the hematopoietic ARS (H-ARS), gastrointestinal ARS (GI-ARS), and neurovascular (NV-ARS) subsyndromes (*5*). Victims exposed to various doses of radiation resulting in H-ARS and GI-ARS have been the interest for the development of MCMs. As of today, the U.S. FDA has approved the use of nine MCMs for H-ARS (Neupogen, Nypozi, Zarxio Neulasta, Udenyca, Stimufend, Ziextenzo, Nplate and Leukine). All of these agents are radiomitigators for postirradiation use (*6–19*) and all stimulate the production of neutrophils except Nplate, which stimulates platelet production. Radiomitigators are needed for the treatment of victims of radiological/nuclear events while radioprotectors for use prior to exposure are required by military personnel and first responders. Though there are several promising agents under development, no MCM for use prior to radiation exposure has yet been approved by the U.S. FDA (*20–24*).

[1] Corresponding author: Vijay K. Singh, Ph.D., Division of Radioprotectants, Department of Pharmacology and Molecular Therapeutics F. Edward Hébert School of Medicine, Uniformed Services University of the Health Sciences, 4301 Jones Bridge Road, Bethesda, MD 20814; email: vijay.singh@usuhs.edu.

Interleukin 11 (IL-11) is a member of the IL-6 family of cytokines with well-characterized biological activities including stimulatory and maturational effects on megakaryocytopoiesis and thrombocytopoiesis, in addition to anti-inflammatory and cytoprotective attributes for hematopoietic progenitors and GI crypts (*25*, *26*). This cytokine also belongs to the gp130 receptor-binding family. IL-11 is the only member that acts on a homodimer of the ubiquitously expressed gp130 co-receptor. Responsiveness of cells to this cytokine is determined by the presence of IL-11Rα present on the cells (*25*). It is also possible that certain cells may not respond to IL-11 due to the lack of IL-11Rα expression (*27*). IL-11 is a drug used for chemotherapy-induced thrombocytopenia (*26*, *28*, *29*). Furthermore, the effects of recombinant human IL-11 (rhuIL-11) on thrombocytopenia and neutropenia have been studied in-depth using various small and large animal models (*26*, *30–32*).

BBT-059 is a long-acting PEGylated IL-11 analog created using site-specific PEGylation technology and modified with a single branched 40 kDa-PEG at a cysteine residue (PEG-*179C) incorporated at the protein's C-terminus. BBT-059 presents its biological effects of stimulating the production of platelets, red blood cells, and to a lesser extent, neutrophils, by binding and activating IL-11R on cells. Hematopoietic and anti-apoptotic effects of IL-11 and BBT-059 on various cells may be important for improving survival after exposure to lethal doses of radiation in the murine model (*26*, *32–34*). Unlike FDA-approved growth factors for ARS, BBT-059 has been found to improve radiation-induced thrombocytopenia as well as neutropenia (*33*, *34*). Furthermore, BBT-059 is also being developed as a potential treatment for thrombocytopenia, myelodysplastic syndromes, bleeding disorders, and acute kidney injury associated with ischemia reperfusion injury (*35*).

The nonhuman primate (NHP) is well known as the gold standard of animal models for developing MCMs following the Animal Rule. This model is also suitable for identifying and validating biomarkers for radiation injury (*36*). Recently, we have reported the pharmacokinetics (PK), pharmacodynamics (PD), and metabolomic results of BBT-059 using unirradiated NHPs (*37*). This study, with 8 NHPs assigned to the 37.5 μg/kg BBT-059 dose group and 6 assigned to the 75 μg/kg BBT-059 dose group, was conducted to investigate the PK/PD of this agent in sublethal-irradiated NHPs. PK and PD studies using unirradiated and irradiated animals are vital steps in radiation MCM development (*38*). Metabolomic studies were performed to determine the various metabolites and pathways stimulated or inhibited by BBT-059 in irradiated animals. We have studied several MCMs under development for metabolomics, including amifostine (*39–42*), BIO 300 (*24*, *43*, *44*), Ex-Rad (*45*), BBT-059 (*37*), and γ-tocotrienol (*23*, *46*, *47*) in murine and NHP models.

As stated above, two different doses of BBT-059 were administered to two different groups of NHPs 24 h after 4 Gy exposure to study the effects on PK/PD and metabolomic profiles. Overall, no adverse reactions were noted in any of the animals administered either dose of BBT-059. Radiation was found to induce metabolomic changes in both treatment groups, specifically in pathways related to steroid hormone biosynthesis, fatty acid activation, and glycerophospholipid metabolism. BBT-059 was found to induce short-term mitigation on a few of these pathways in one dose group or the other, but only commonly mitigated damage in the linoleate metabolism pathway. We have previously investigated metabolomic profiles in NHPs that were administered three different doses of BBT-059 without irradiation, and these results were compared with the current study to determine the effects of BBT-059 in combination with radiation (*37*).

MATERIALS AND METHODS

Experimental Design

The primary objective of this study was to investigate the PK/PD profile of BBT-059 in NHPs exposed to total-body cobalt-60 γ radiation. Based on the results of the PK/PD study conducted in NHPs without irradiation, the 37.5 and 75 μg/kg doses were selected for this experiment and were evaluated in animals exposed to total-body sublethal radiation (4 Gy). A total of 14 NHPs were used in this study. Eight animals were randomly assigned to the 37.5 μg/kg treatment group, while six animals were assigned to the 75 μg/kg group. Single subcutaneous (sc) doses of BBT-059 were administered on day 1 (based on the body weight, total volume not to exceed 1.33 mL), which was 24 h postirradiation (Fig. 1). The doses of BBT-059 were allometrically scaled from studies conducted using a murine model, which exhibited encouraging results and were also used in a recently reported NHP PK/PD study without irradiation (*33*, *34*, *37*). We used allometric scaling to extrapolate doses from the murine model to NHPs using the FDA Center for Drug Evaluation and Research document (*48*). A single SC injection of 300 μg/kg of agent in mice was found to be safe (*33*) and is equivalent to a dose of 75 μg/kg for NHPs. The animals were observed for 60 days postirradiation to conduct various investigations. The blood sample collection and study design are presented in Fig. 1. It is important to note that both treatment groups were exposed to radiation, and there was no group that was exposed to radiation and was not administered a drug. Due to the complexity of the experimental timeline, the time points are referred to as follows: pre-irradiation (baseline), after irradiation but pre-drug administration (irradiated baseline), and after irradiation and after drug administration time points (after irradiation).

Animals

A total of 14 naïve rhesus macaques (*Macaca mulatta*) seven males and seven females, varying between 4.08 – 6.41 years of age and weighing 4.0–7.6 kg, were obtained from PrimGen (Lehigh Acres, FL) and quarantined for at least 35 days before the experiment. Animal quarantine, exclusion criteria, housing, health monitoring, care, and enrichment during the experimental period have been described earlier (*49*, *50*). Animals were stratified by gender and body weight, which increased during the quarantine period, using Provantis software (Philadelphia, PA). They were then assigned to different treatment groups, and all rhesus macaques had unique identification numbers by four-digit tattoo.

Irradiation

On day 0, animals received a midline dose of 4.0 Gy ^{60}Co-γ bilateral radiation at a dose rate of 0.6 Gy/min. Animals were transported from the vivarium to the high-level cobalt facility, placed into a standard housing cage staging area, and prepared for irradiation as described previously (*51*). To deliver the precise dose of radiation, the abdominal lateral separations of the animals were measured one

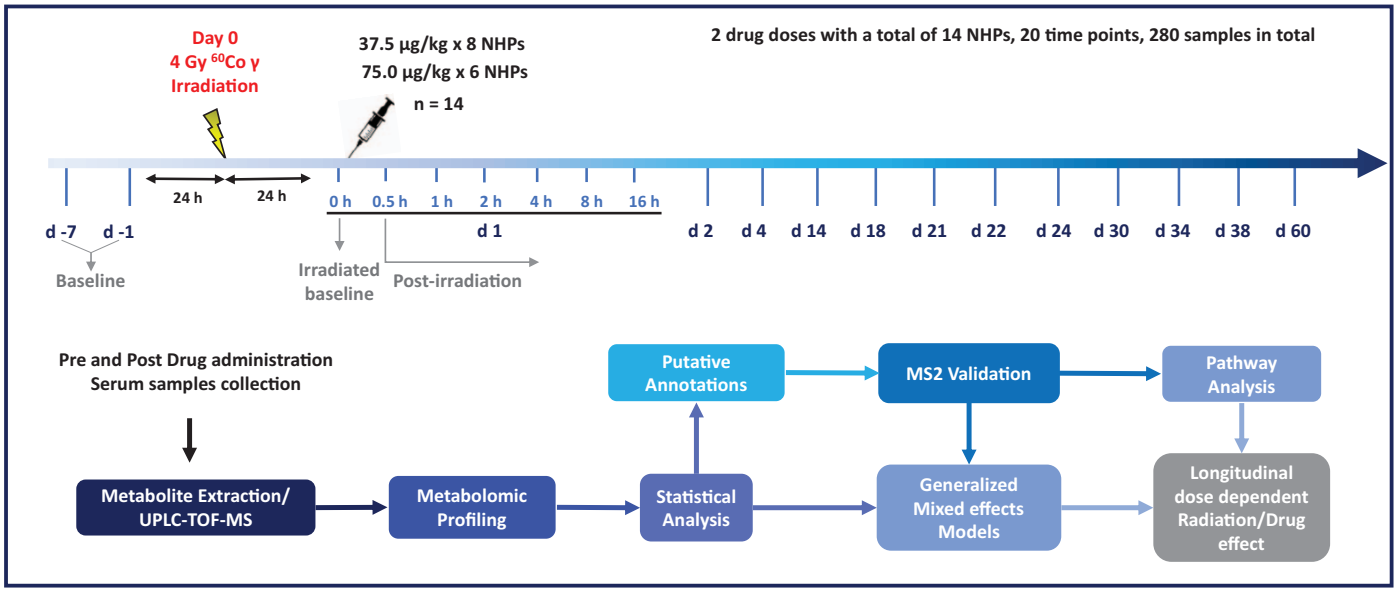

FIG. 1. Experimental design of the NHP study with irradiation to investigate the effect of BBT-059 administration on PK/PD and metabolomics.

week before irradiation, and animals were paired based on the similarity of their lateral separations. Animals having 1 cm or more difference in lateral separation were irradiated separately. The radiation field in the area of the NHP location was uniform within ± 1.5%. Dose measurements and calibrations were based on alanine/electron paramagnetic resonance system (*52*, *53*). All irradiation procedures and dosimetry are discussed in detail in the literature (*49*, *51*).

Cage-side Animal Observations

Animals were observed at least twice each day for the entirety of the quarantine and study periods. Any unexpected observations were reported to the veterinarian for further assessment. Starting on day 1, clinical observations were recorded once a day. Clinical observations included, but were not limited to, sustained vomiting or diarrhea, dyspnea, cyanosis, anorexia, weakness, lack of response to stimuli, seizures, paralysis, repeated self-trauma, severe skin infections, and non-healing wounds. During days 10 through 20 postirradiation (also known as the critical period), health checks were performed three times per day (*50*). All NHPs participated in the environmental enrichment program. This program allowed the animals to be housed in such a manner that provided them with visual and auditory contact with the other animals. All animals were provided with a perch or hammock in the cage, a mirror, and a jingle-type toy hanging on the outside of the cage. Additionally, animals were provided a variety of manipulanda to provide them with an opportunity to perform species-specific activities such as foraging. One or more of the devices/toys were available to all NHPs at all times. The animals were evaluated for the following parameters at least three times per week: weight, body temperature, fecal consistency, respiratory rate, heart rate, and overall health assessment (*49*). All observations were appropriately documented in the animals' medical records.

Vital Signs

Vital signs, including blood pressure, heart rate, temperature, and body weight, were measured on the days of blood sample collection. Blood pressure was measured using a cuff that was secured around the upper arm of the NHP connected to a vital sign monitor (Surgivet 3 Parameter Advisor; Smiths Medical, Dublin, OH), which used the machine's non-invasive blood pressure program. Heart rate was measured via pulse oximetry or palpation. Microchips (Bio-Medic Data Systems; IPTT 300 transponder) were implanted SC (under ketamine anesthesia) between the shoulder blades of each animal one week prior to irradiation to record body temperatures, and body weights were measured using a jump box scale. For blood collection, NHPs were restrained in a chair using the pole and collar technique to avoid repeated sedation. Under such conditions, it was not feasible to measure respiratory rate since it involves counting the number of breaths at rest.

Drug Preparation and Administration

The drug administration was discussed in an earlier study without irradiation (*37*). The injection site was prepared as previously described (*49*). Drug was administered by SC injection between the shoulder blades. Injection sites were monitored for any adverse reactions for the next 24 h after drug administration.

Blood Sample Collection

Blood was collected either from saphenous or cephalic vein as described earlier (*54*). The desired volume of blood was collected with a 3 mL disposable luer-lock syringe with a 25-gauge needle. Whole blood was collected in ethylenediaminetetraacetic acid (EDTA) tubes for complete blood counts (CBC) and PK analysis. Whole blood was transferred to Capiject serum separator tubes and allowed to clot for 30 min, then centrifuged (10 min, 400 × g) for serum separation for biochemistry and PD analysis.

Hematology (CBC) Analysis

To analyze CBCs, blood samples were analyzed using a Heska Element HT5 hematology analyzer (Colorado, DE). Various parameters evaluated included white blood cell count, red blood cell count, hemoglobin, hematocrit, mean corpuscular volume (MCV), mean cell hemoglobin (MCH), mean corpuscular hemoglobin concentration (MCHC), and platelet, neutrophil, lymphocyte, monocyte, eosinophil, and basophil counts as described earlier (*55*).

Blood Biochemistry Evaluation

For serum biochemistry, samples were shipped to a reference laboratory, VRL Diagnostics (Gaithersburg, MD), for analysis. Parameters that were evaluated included: albumin, alkaline phosphatase, alanine aminotransferase (ALT), aspartate aminotransferase (AST), blood urea nitrogen (BUN), calcium, chloride, cholesterol, creatine

kinase (CK), creatinine, glucose, phosphorus, potassium, sodium, total bilirubin, and total protein.

Multiplex Analysis of Cytokines

Serum samples were analyzed with a Luminex 200 analyzer (Luminex Corp, Austin, TX) to detect cytokines, chemokines, and growth factors using custom-made 48-plex multiplex kits (Bio-Rad Laboratories, Hercules, CA). A comprehensive list of these cytokines was mentioned previously (*55*). Cytokine concentrations (pg/mL) were determined by fluorescence intensity, and quantification was performed using the Bio-Plex Manager software, version 6.1 (Bio-Rad Inc.) (*56*).

PK Analysis

Bioanalysis of plasma samples to measure BBT-059 concentrations was performed using a commercially available ELISA kit, RayBio Human IL-11 ELISA (RayBiotech, ELH-IL-11, Peachtree Corners, GA), a sandwich-based ELISA assay described previously (*37*). Serial dilutions of BBT-059 were used as the reference standards in the ELISA. The calculated concentration of each BBT-059 test sample in the ELISA was then multiplied by the appropriate plasma dilution factor for the final BBT-059 plasma concentration. The lower limit of quantification for BBT-059 in the ELISA was 16.4 ng/mL; plasma samples below this level were assigned a value of 0 when determining group means. PK parameters were estimated for each animal using Phoenix 64 WinNonlin pharmacokinetic software Build 8.1.0.3530 (Certara L.P.). A non-compartmental approach consistent with the SC route of administration was used for parameter estimation. The area under the protein concentration versus time curve ($AUC_{(0\text{-}t)}$), $AUC_{(0\text{-}t)}$ divided by the dose administered ($AUC_{(0\text{-}t)}/D$), the area under the concentration versus time curve from time zero to infinity ($AUC_{(0\text{-}\infty)}$), $AUC_{(0\text{-}\infty)}$ divided by the dose administered ($AUC_{(0\text{-}\infty)}/D$), the maximum plasma drug concentration (C_{max}), time to peak plasma concentration (T_{max}), the apparent volume of distribution during the terminal elimination phase (V_z/F), and the half-life ($T_{1/2}$) of the drug were calculated by the WinNonlin program.

Serum Metabolomics Using UPLC QTOF Analysis

Whole blood was collected in a serum separator tube and allowed to clot for a minimum of 30 min after collection. The serum was separated and placed in a cryogenic storage tube and stored at –80°C until analysis. Before sample preparation for LC-MS analysis, the sequence of samples was randomized to avoid any bias. Detailed methods for metabolite extraction and LC-MS analysis are described in detail in our recent publications using NHP samples (*57*, *58*). A comprehensive list of the metabolites screened for in this study are listed in Supplementary Table S1[2] (https://doi.org/10.1667/RADE-24-00219.1.S1).

Data Processing and Statistical Analysis

For vital signs, CBC, blood chemistry, and cytokine data, mean values with standard errors were reported. One-way analysis of variance (ANOVA) with a Tukey post-hoc test was used to detect significant differences between treatment groups at each timepoint. Additionally, repeated measures two-way ANOVA tests with Bonferroni corrections were also performed for vital signs, CBC, and cytokine data to assess the effects of drug administration over the course of the study within each treatment group. The baseline was compared to post-drug administration timepoints to assess significant differences over time within treatment groups. Statistical software SPSS version 22 (IBM, Armonk, NY) was used for all statistical analyses, and p-values less than 0.05 were considered statistically significant.

Metabolomics data was log transformed and scaled following feature detection. Statistical analyses were then performed to follow longitudinal changes in metabolomic profiles and any changes in the phenotype. First, untargeted metabolomics raw data files were converted to NetCDF file format using the Databridge tool in MassLynx (Waters Corporation, Milford, MA). All parameters for peak picking were optimized by the IPO (Isotopologue Parameter Optimization) R package (*59*) and were then processed by the XCMS package (*60*). All data was then normalized based on both the internal standard and the QC-RLSC (QC robust LOESS signal correction (*61*)). Other details of data analysis have been described previously (*37*, *43*). Statistical comparisons were performed on metabolite and pathway data for the 37.5 and 75 μg/kg treatment groups to assess differences between the baseline and irradiated baseline or post-irradiation time points (Supplementary Tables S2–S5; https://doi.org/10.1667/RADE-24-00219.1.S1).

[2] Editor's note. The online version of this article (DOI: https://doi.org/10.1667/RADE-24-00219.1) contains supplementary information that is available to all authorized users.

RESULTS

A drug safety assessment and toxicity profile of BBT-059 were completed through the analysis of metabolomic data, in addition to vital signs, CBC, blood chemistry, cytokine, and PK/PD studies. No treatment group experienced adverse reactions to BBT-059 administration. The study design is presented in Fig. 1.

Minimal Differences Were Observed in Vital Signs Between the Two Treatment Groups

Across all vital signs measured (heart rate, temperature, blood pressure and body weights), variation was observed for each parameter and no overall trends were noted. Animals in both treatment groups experienced a decrease in body weight after irradiation, but recovered to slightly higher body weights compared to the baseline by the end of the study. Significant differences were observed in temperature, heart rate, weight, and diastolic blood pressure between the two treatment groups at a few isolated time points; however, no overall trend was observed. Statistical analysis was also performed to assess intergroup differences over time (Supplementary Table S6; https://doi.org/10.1667/RADE-24-00219.1.S1). Minimal significant differences were observed between the baseline and the irradiated baseline or post-irradiation time points within treatment groups, suggesting irradiation and drug administration had minimal effects on vital signs. Results for vital signs for this study can be viewed in Supplementary Fig. S1 (https://doi.org/10.1667/RADE-24-00219.1.S2).

Radiation Induced Decreases in CBCs Regardless of Treatment Group

Radiation had similar effects on CBCs in both treatment groups regardless of BBT-059 dose. All parameters decreased upon irradiation in both treatment groups. A few significant differences were noted at a few time points between treatment groups. However, these significant differences did not typically follow a trend, apart from one parameter, lymphocyte counts decreased after irradiation and were generally higher in the 75 μg/kg treatment group upon recovery, beginning around day 6 and continuing throughout the remainder of the study. Statistical comparisons were also performed to determine

TABLE 1
Summary of BBT-059 Single Dose PK Parameters in NHPs[a]

Dose	Animals	T_{max} (h)	C_{max} (ng/mL)	$AUC_{(0\text{-}t)}$ (ng h/mL)	AUC(0-t)/D (hr*kg*ng/mL/μg)	$AUC_{(0\text{-}inf)}$ (ng h/mL)	AUC(0-inf)/D (hr*kg*ng/mL/μg)	V_z/F (mL/kg)	$T_{1/2}$ (h)
37.5 μg/kg	All	12 ± 7	192 ± 50	5,749 ± 1,727	153 ± 46	7,148 ± 1,495	191 ± 40	166 ± 69	21 ± 8
	Males	10 ± 4	179 ± 60	5,018 ± 1,402	134 ± 37	6,669 ± 1,361	178 ± 36	191 ± 96	23 ± 11
	Females	13 ± 9	206 ± 43	6,480 ± 1,889	173 ± 51	7,626 ± 1,658	203 ± 44	141 ± 20	20 ± 2
75 μg/kg	All	11 ± 7	258 ± 66	9,109 ± 2,723	121 ± 36	10,989 ± 3,167	147 ± 42	307 ± 100	29 ± 7
	Males	13 ± 9	291 ± 56	10,529 ± 3,108	140 ± 41	12,057 ± 3,898	161 ± 52	276 ± 135	28 ± 8
	Females	8 ± 0	225 ± 66	7,690 ± 1,683	103 ± 22	9,921 ± 2,542	132 ± 34	337 ± 63	31 ± 8

[a] Data are mean and standard deviations for 8 animals in the 37.5 μg/kg group (4 males, 4 females), and 6 animals in the 75 μg/kg group (3 males, 3 females).

significance over time within treatment groups (Supplementary Table S7; https://doi.org/10.1667/RADE-24-00219.1.S1). Significant differences were noted when comparing the baseline to the post-irradiation time points in a majority of parameters, suggesting irradiation induced significant dysregulation in CBC parameters. CBC results can be viewed in Supplementary Figs. S2 and S3 (https://doi.org/10.1667/RADE-24-00219.1.S2).

Minimal Radiation-induced Effects Were Noted in Blood Chemistry Parameters

Both treatment groups followed similar trends for most blood chemistry parameters evaluated. A few parameters exhibited consistently higher or lower concentrations in one treatment group. Most notably, the concentration of albumin was significantly higher at several time points (16 h and days 3,14, and 60 postirradiation) throughout the study in the 37.5 μg/kg group. In contrast, the 75 μg/kg group demonstrated higher concentrations of alanine aminotransferase (ALT), aspartate aminotransferase (AST), cholesterol, and creatine kinase at a majority of time points throughout the study period with statistical significance at various time points. Alkaline phosphatase (ALP), blood urea nitrogen (BUN), calcium, chloride, creatinine, glucose, phosphorus, potassium, sodium, total bilirubin, and total protein displayed fluctuating concentrations between the two dose groups, with few or no significant differences. Parameter concentrations tended to peak around 16 h to 3 days after irradiation but returned to baseline levels by the study endpoint. Additional statistical comparisons were performed to assess differences between baseline and post-irradiation time points within treatment groups (Supplementary Table 8; https://doi.org/10.1667/RADE-24-00219.1.S1). Significant differences were noted in ALB for both treatment groups, and calcium, sodium, and globulin in the 37.5 μg/kg group, along with a few other isolated parameters. Chemistry results can be viewed in Supplementary Figs. S4–S6 (https://doi.org/10.1667/RADE-24-00219.1.S2).

Minimal Differences in Cytokine Concentrations Were Observed in Either Treatment Group

A majority of the cytokine concentrations followed similar trends between the two treatment groups and fluctuated greatly throughout the 60-day study period. The concentrations of a few cytokines including IL-16, IL-4, PDGF-BB, MCP-1, IL-18, and LIF increased shortly after irradiation and drug administration and then slowly decreased back toward baseline measurements; PDGF-BB concentrations, however, increased in the 75 μg/kg group beginning on day 30 and continued that trajectory until the end of the study. Other cytokines such as SCF, IL-12p40, and M-CSF fluctuated minimally from baseline concentrations in either treatment group. As was performed for the other parameters, additional statistical comparisons to address intergroup comparisons over time were performed (Supplementary Table S9; https://doi.org/10.1667/RADE-24-00219.1.S1). IL-16, TNF-α, SCF, PDGF-BB, MCP-1, IL-12p40, SDF-1α, and LIF concentrations were mostly higher in the 75 μg/kg treatment group; however, this trend was present in baseline measurements and mostly continued throughout the study in these parameters apart from a few exceptions. Concentrations of certain cytokines including IL-8, SDF-1α, TRAIL, HGF, and IL-9 fluctuated later in the study, but generally returned to baseline levels by the end of the study. Cytokine concentrations over time can be viewed in Supplementary Figs. S7–S9 (https://doi.org/10.1667/RADE-24-00219.1.S1).

PK Results

The results of the PK analysis can be viewed in Table 1. PK analysis of plasma samples showed that plasma concentrations of BBT-059 were highest within the first 2 days after drug administration, and declined gradually thereafter (Fig. 2). C_{max}, the observed maximum plasma concentration of the drug, and the plasma concentration time profiles, $AUC_{(0\text{-}t)}$ and $AUC_{(0\text{-}inf)}$, increased by less than double with a double dose of BBT-059. The values of C_{max}/dose, $AUC_{(0\text{-}t)}$/dose, and $AUC_{(0\text{-}inf)}$/dose decreased with the higher dose of BBT-059 while the terminal half-life ($T_{1/2}$) of BBT-059 increased with the higher dose. T_{max} was similar in both dose groups. The apparent volume of distribution, V_z/F, was approximately twofold greater for the 75 μg BBT-059 dose (307 ± 100 mL/kg) compared to the 37.5 μg BBT-059 dose (166 ± 69 mL/kg). The V_z/F values suggest BBT-059 is largely restricted to the blood/plasma

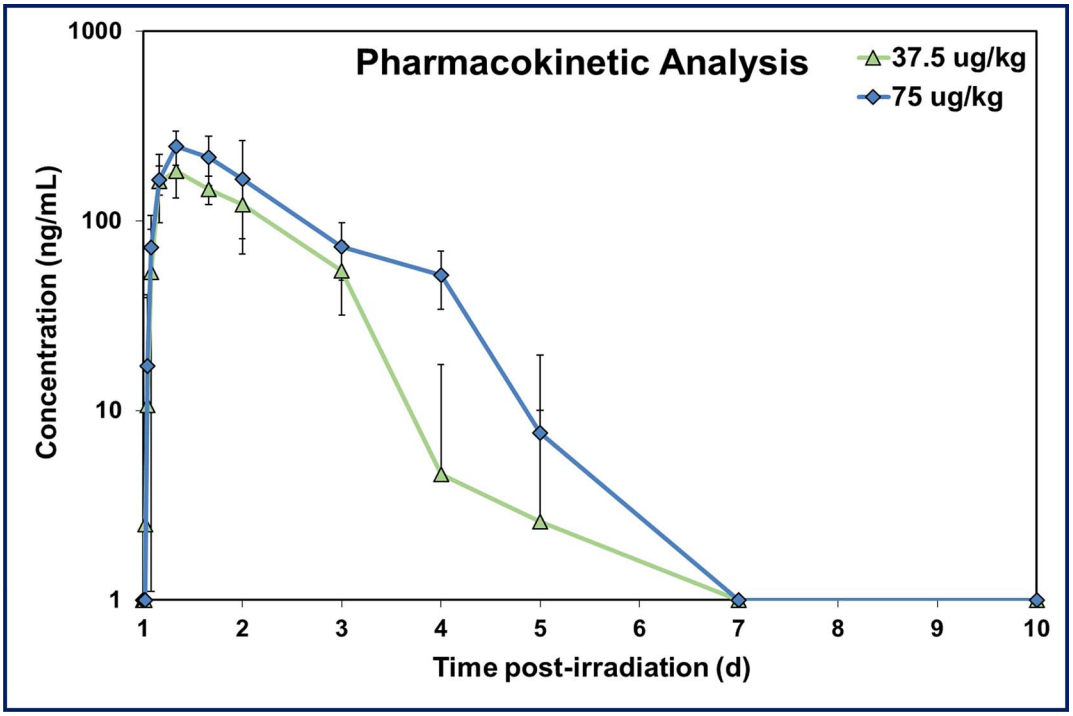

FIG. 2. Pharmacokinetic analysis to evaluate BBT-059 concentration after irradiation and subsequent drug administration (37.5 μg/kg and 75 μg/kg). Data are means ± standard deviations.

compartment. Pharmacokinetic parameters for males and females within a dose group were similar ($P \geq 0.24$ for all parameters using a two-tailed t-test).

Radiation Induced a Majority Downregulation in Metabolites Analyzed in Both Treatment Groups

Radiation-induced metabolite dysregulation was observed in both treatment groups, and the degree of dysregulation fluctuated throughout the study for both treatment groups (Fig. 3). Dysregulation that was not mitigated by BBT-059 administration was assessed by the presence of significance when comparing the baseline to post-irradiation time points. Particular attention was paid to the irradiated baseline (which was 24 h postirradiation, yet pre-drug administration), to assess the effects of radiation (Fig. 4A and B). Some early, short-term radiomitigation was afforded by either dose of BBT-059 at the 4 h time point (Fig. 4C and D). However, this radiomitigation was short-lived, and ended after approximately day 4 postirradiation in both treatment groups (Fig. 4E and F). Both treatment groups experienced a major downregulation of metabolites throughout the study, with the 75 μg/kg dose group demonstrating a greater degree of downregulation than the 37.5 μg/kg dose group. However, at a few time points, specifically 2 and 4 h postirradiation in the 37.5 μg/kg treatment group, a majority of the metabolites were upregulated compared to the baseline.

Minimal consistency in terms of dysregulation patterns in specific metabolomic pathways were noted between the two treatment groups; more specifically, dysregulation of certain pathways was limited to one treatment group. In the 37.5 μg/kg dose group, notable pathways including tyrosine metabolism and the valine, leucine, and isoleucine degradation pathways were dysregulated by radiation exposure; in the 75 μg/kg dose group, the fatty acid activation, fatty acid metabolism, and androgen and estrogen biosynthesis and metabolism pathways were dysregulated. However, the C21-steroid hormone biosynthesis and metabolism, fatty acid activation, and linoleate metabolism pathways were commonly dysregulated by radiation in both treatment groups at several time points (Fig. 5A–C).

Several metabolites were commonly and significantly dysregulated by radiation exposure at a majority of the time points assessed in both treatment groups including monoisobutyl phthalic acid, N-methylhydantoin, ganoderic acid L, erinacine P, [6]-dehydrogingerdione, 2,6-di-tert-butylbenzoquinone, methyl dihydrophaseate, 2,3-dimethyl-2-cyclohexen-1-one, azelaic acid, 3-hydroxydodecanoic acid, and petasinine. Other metabolites were uniquely dysregulated in only one BBT-059 treatment group or the other, octanoic acid, N-trimethyl-2-aminoethylphosphonate, along with lipids PA(14:0/18:4(6Z,9Z,12Z,15Z)) and PA(14:1(9Z)/18:4(6Z,9Z,12Z,15Z)) in the 37.5 μg/kg dose group, and 5-nonyltetrahydro-2-oxo-3-furancarboxylic acid and asparaginyl-tryptophan in the 75 μg/kg dose group.

BBT-059 Administration Induced Early Radiomitigation to Specific Metabolites and Pathways

To assess whether BBT-059 administration mitigated radiation-induced damage, the presence of significant dysregulation at the irradiated baseline was examined and compared to the absence of significant dysregulation at the

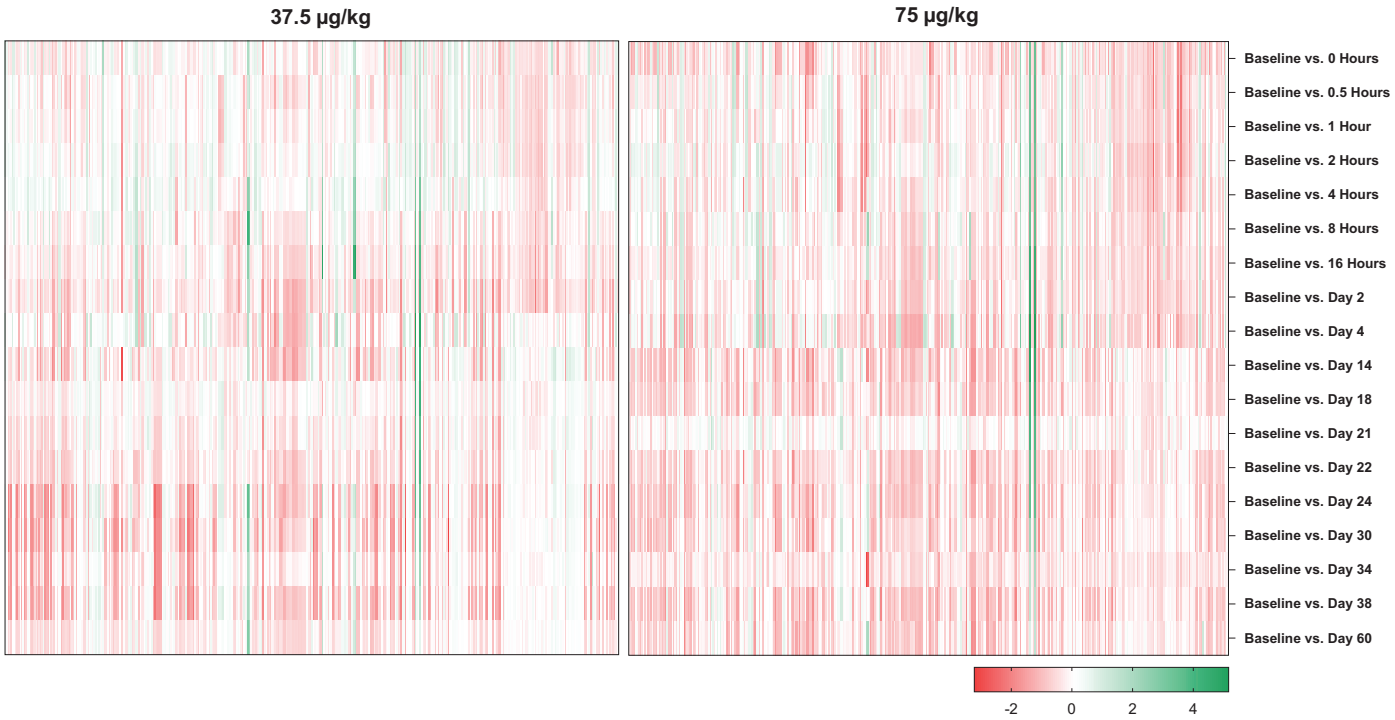

FIG. 3. Heatmaps comparing the metabolites detected in the 37.5 and 75 µg/kg treatment groups. The Baseline vs. 0 Hours comparison represents the effects of radiation. Overall, both treatment groups experienced a majority downregulation after 4.0 Gy total-body γ irradiation.

post-irradiation time points. The number of significantly dysregulated metabolites decreased in both treatment groups after either dose of BBT-059 was administered, and this mitigatory effect seemed to last until day 2 in the 37.5 µg/kg dose group and day 4 in the 75 µg/kg dose group, at which point dysregulation returned to around irradiated baseline counts and continued to fluctuate throughout the remainder of the study.

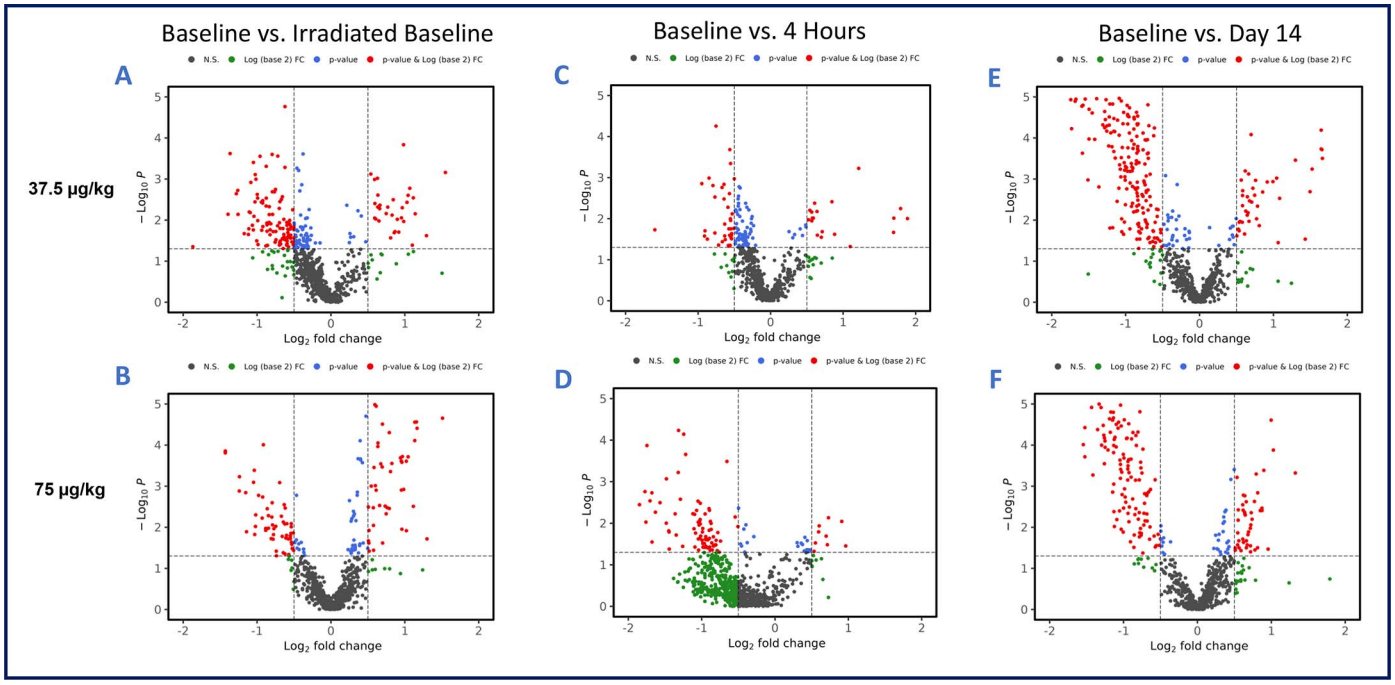

FIG. 4. Volcano plots illustrating differential expression comparing the baseline (pre-irradiation and pre-drug administration) to the irradiated baseline (24 h postirradiation) (panels A and B), 16 h postirradiation (panels C and D), and day 14 postirradiation (panels E and F) in the 37.5 µg/kg and 75 µg/kg dose groups, respectively.

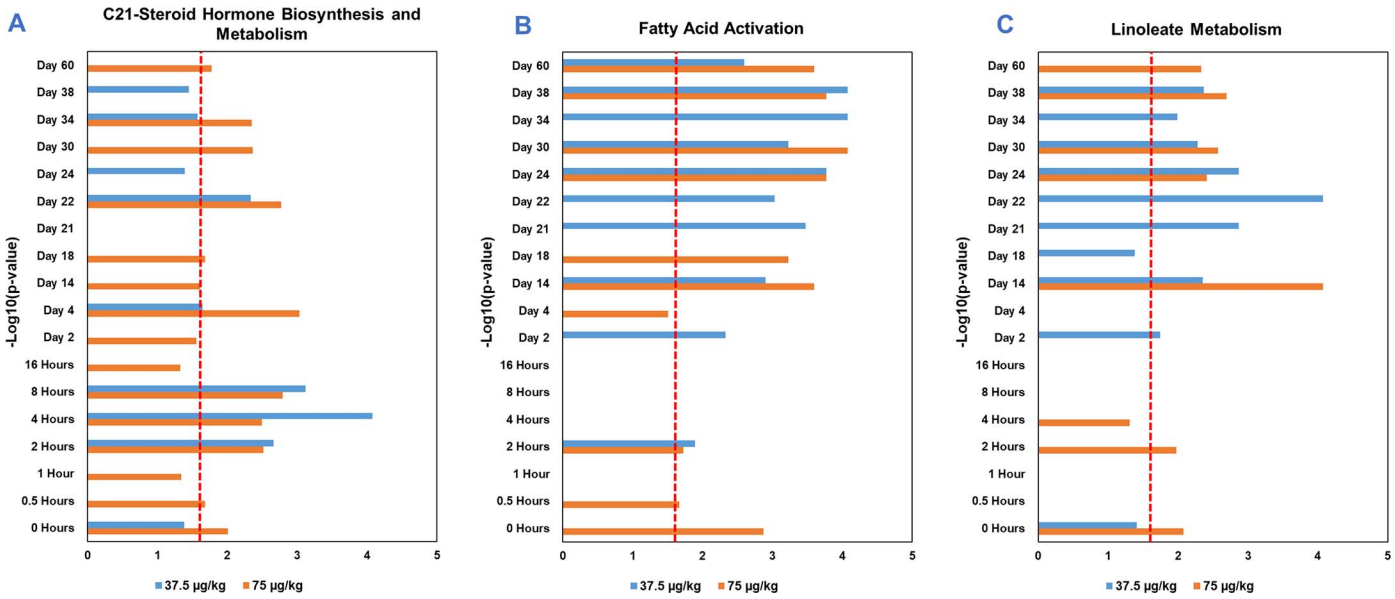

FIG. 5. Notable metabolic pathways were dysregulated by radiation including the C21-steroid hormone biosynthesis and metabolism pathway (panel A), the fatty acid activation (panel B), and the linoleate metabolism pathway (panel C). Dysregulation fluctuated throughout the study for each pathway; however, BBT-059 afforded some early, short-term mitigative effects from 0.5 h to approximately day 4 in either treatment group.

Dysregulation of other pathways including the bile acid biosynthesis, β-alanine metabolism, histidine metabolism, squalene and cholesterol biosynthesis, selenoamino acid metabolism, proponoate metabolism, and C21-steroid hormone biosynthesis and metabolism pathways were initially mitigated by a 37.5 µg/kg dose of BBT-059, but dysregulation persisted at a few time points (Supplementary Table S3; https://doi.org/10.1667/RADE-24-00219.1.S1). As for the 75 µg/kg group, pathways including the de novo fatty acid biosynthesis, fatty acid metabolism, vitamin (A) retinol metabolism, linoleate metabolism, xenobiotics metabolism, and arachidonic acid metabolism were initially dysregulated in the irradiated baseline, and were then mitigated by BBT-059 treatment. Linoleate metabolism was the only pathway that was dysregulated in the irradiated baseline group that was then resolved after administration of either dose of BBT-059. As for specific metabolites, dysregulation to 2-Methyl-2-phenyl-undecane, Polyprenol, 11-Dehydrocorticosterone, and octadecadienoate (n-C18:2) were restored by either dose of BBT-059.

DISCUSSION

PEGylated interleukin-11 (BBT-059) is currently being developed as a radiomitigator, or an MCM administered after radiation exposure to mitigate radiation-induced damage, and has exhibited the potential to stimulate hematopoietic cell production (*62*, *63*). In this study, a 37.5 µg/kg (n = 8) and 75 µg/kg (n = 6) dose of BBT-059 was administered to NHPs 24 h after exposure to a sublethal dose of 4.0 Gy total-body γ-irradiation. Various data were collected to evaluate the potential mitigative effects of BBT-059. Some radiation-induced changes were observed in CBCs, while minimal changes were observed among vital signs, blood chemistry, and cytokine profiles. Overall, minimal differences were observed between BBT-059 treatment groups in each of these parameters. PK analysis showed that the $T_{1/2}$, C_{max}, $AUC_{(0\text{-}t)}$, and $AUC_{(0\text{-}inf)}$ increased with increasing BBT-059 dose, although the manner was not proportional to dose. Comparing these results to those from a SC dosing PK study of 37.5 and 75/kg µg BBT-059 in non-irradiated rhesus NHPs [37], it appears that exposure to radiation results in slightly lower BBT-059 C_{max}, $AUC_{(0\text{-}t)}$, and $AUC_{(0\text{-}inf)}$ levels, but higher $T_{1/2}$ values. BBT-059 V_z/F values were approximately two-fold greater in irradiated animals compared to non-irradiated animals, suggesting greater tissue penetration in irradiated animals, although in both cases the drug was still largely confined to the blood/plasma compartment. A caveat to these conclusions is the fact that the experiments were performed at different times. In brief, the above observations suggest that the drug doses used in this study do not cause any adverse effects on the vital signs, CBCs, chemistry, or cytokine profiles of the recipients, and ultimately have a good safety profile.

One important factor to consider when assessing BBT-059/IL-11 plasma concentrations is that human and NHP IL-11 share 94% amino acid homology (*37*, *64*). Due to this fact, the ELISA kit used in this study to assess cytokine profiles could not discriminate between human IL-11 and BBT-059, apart from sensitivity. The 0 ng/mL BBT-059 standard, the irradiated baseline, and the plasma collected at later time points were negative for BBT-059 (below the limit of quantification of 16.4 ng/mL). Consequently, it is possible that NHP IL-11 could have been detected by the human IL-11 ELISA kit, and plasma samples determined

to contain BBT-059 could be measuring a combination of BBT-059 and endogenous NHP IL-11. Therefore, it can reasonably be assumed that the plasma samples that were determined to be below the lower limit of quantification of BBT-059 are also below the lower limit of detection of NHP IL-11. Ultimately, we have not measured affinities of human IL-11 or BBT-059 for mouse, human, or NHP IL-11 receptors, so the potential receptor affinity differences were not considered when allometric scaling of drug doses between mice and NHPs was performed. There is a high degree of amino acid similarity between human, NHP, and murine IL-11 proteins. As previously mentioned, human and NHP IL-11 share 94% amino acid similarity, while human and mouse IL-11 share 87.5% amino acid similarity, and mouse and NHP IL-11 share 83.5% amino acid similarity (*64*). The higher amino acid similarity between human and NHP IL-11 proteins compared to human and mouse IL-11 suggests that an allometrically scaled dose of BBT-059 may be somewhat more potent in NHPs than in mice, and that physiological responses observed for BBT-059 in NHPs may be more predictive of the expected responses of the drug in humans. Further studies will be needed to better evaluate the physiological responses of the different doses of BBT-059 in mice, NHPs, and humans.

Plasma metabolomic profiles were also assessed at various time points throughout the study. Radiation exposure has been previously shown to induce dysregulation to metabolomic profiles, which was also observed in this study (*65–67*). Pathways that are highly sensitive to radiation were dysregulated in this study at a majority of the time points analyzed. Some examples include the C21-steroid hormone biosynthesis and metabolism pathway, glycerophospholipid metabolism, and fatty acid activation pathways. A few metabolites were also commonly dysregulated in both BBT-059 treatment groups including ganoderic acid L, [6]-dehydrogingerdione, 2,6-di-tert-butylbenzoquinone, and 3-hydroxydodecanoic acid. Notably, 3-hydroxydodecanoic acid has been associated with fatty acid disorders (*68*), and further supports the notion that irradiation induces dyslipidemia.

Dysregulation to some of these pathways was mitigated by one dose of BBT-059 but not the other; i.e., the C21-steroid hormone biosynthesis and metabolism pathway was not affected in the 37.5 μg/kg treatment group, but this was not the case for the 75 μg/kg treatment group. However, radiation-induced metabolomic dysregulation was mitigated for one notable metabolite in this pathway in both treatment groups: 11-dehydrocorticosterone. Notably, the linoleate metabolism pathway was the only pathway commonly mitigated by either dose of BBT-059. One metabolite, octadecadienoate (n-C18:2), was linked to this pathway and followed a similar trend in both treatment groups.

During the last few years, we have extensively studied metabolomic changes induced by lethal doses of ionizing radiation (*69*). We investigated altered metabolites in both biofluids and tissue samples using murine (*39–41*) and NHP (*57*, *58*, *66*, *70–72*) models that received ^{60}Co γ total-body irradiation, NHPs exposed to partial-body radiation with LINAC-derived photons (*58*), and clinical patients exposed to LINAC-derived photons (X rays) (*73*). In addition, we have studied metabolites in pre-terminal samples from moribund γ-irradiated NHPs to identify the biomarkers that may be valuable for triage purposes (*57*). Various MCMs that are being developed for prophylactic or mitigative use were also used to assess the effects on metabolomics in irradiated and unirradiated animals (*37*, *39–41*, *43–47*, *58*). The studies with irradiated animals using murine and NHP models demonstrate that alterations in metabolites induced by acute exposure to ionizing radiation can be mitigated to some extent by MCMs (*39–41*, *45*, *46*, *58*). We have also studied a multi-platform metabolomics [LCMS and nuclear magnetic resonance (NMR)] to comprehensively characterize the temporal changes in metabolite levels in samples collected from mice and NHPs after γ irradiation, which suggested a unique physiological change that is independent of radiation dose or species (*39*).

An earlier PK/PD study was performed in NHPs, which analyzed the effects of a single SC administration of 37.5, 75, or 150 μg/kg dose of BBT-059 without irradiation. Overall, some similarities were observed between these two studies in terms of pathways activated or mitigated by BBT-059 administration. In the previous study, the C21-steroid hormone biosynthesis pathway was found to be significantly stimulated by the administration of all doses of BBT-059. In the current study, the C-21 steroid hormone biosynthesis pathway was significantly dysregulated by radiation exposure in both treatment groups; however, dysregulation resolved upon administration of 37.5 μg/kg BBT-059, while dysregulation persisted with the 75 μg/kg dose. The C-21 steroid hormone biosynthesis pathway has been shown to be highly sensitive to ionizing radiation, as has been demonstrated in many of our previous studies. Notably, 11-dehydrocorticosterone, a key metabolite in this pathway, was found to be significantly upregulated in the previous study, regardless of the three BBT-059 doses administered, and was also significantly mitigated in this study by either dose of BBT-059. This corticosteroid is believed to be upregulated in inflammatory conditions, where it exhibits anti-inflammatory activity (*74*). Notably, a recent study has been performed comparing metabolomic changes induced by two doses of 2.0 Gy total-body irradiation in leukemia patients and a single dose of 7.2 Gy total-body irradiation in NHPs which demonstrated overlapping perturbations in steroidogenesis and steroid hormone biosynthesis and metabolism (*73*). Taken together, these results strongly indicate these pathways need further investigation for potential translation into clinical medicine.

One important aspect of this study is that although the irradiated baseline reflects the effects of radiation, it is impossible to definitively determine the effects of radiation over time or the mitigative effects of drug administration due to the absence of an irradiated control group in this study. In this study, the irradiated baseline, which was 24 h

postirradiation, was used to assess radiation-induced changes. However, it is important to note that radiation-induced changes can manifest after 24 h. Therefore, the irradiated baseline only provided a glimpse of radiation-induced changes. The ultimate purpose of this study was to determine the pharmacokinetic and pharmacodynamic signatures of BBT-059 administration, and as such, a control group was not included per the study design. Due to these limitations, additional studies must be performed investigating the radiomitigative effects of BBT-059 with an irradiated control group and a greater sample size.

SUPPLEMENTARY MATERIALS

Supplementary Table S1. The complete list of metabolites are screened in this study.

Supplementary Table S2. Statistical comparisons were performed comparing metabolite profiles at the baseline (pre-irradiation and pre-drug administration) to the irradiated baseline (24 h postirradiation) and the postirradiation times in the 37.5 μg/kg treatment group.

Supplementary Table S3. Statistical comparisons were performed comparing metabolite profiles at the baseline (pre-irradiation and pre-drug administration) to the irradiated baseline (24 h postirradiation) and the postirradiation times in the 75 μg/kg treatment group.

Supplementary Table S4. Pathway analysis was performed by comparing metabolite profiles at the baseline (pre-irradiation and pre-drug administration) to the irradiated baseline (24 h postirradiation) and the postirradiation times in the 37.5 μg/kg treatment group.

Supplementary Table S5. Pathway analysis was performed by comparing metabolite profiles at the baseline (pre-irradiation and pre-drug administration) to the irradiated baseline (24 h postirradiation) and the postirradiation times in the 75 μg/kg treatment group.

Supplementary Table S6. Repeated measures two-way ANOVA tests were performed to assess the effects of drug administration on vital signs data by comparing baseline measurements to post-drug administration timepoints.

Supplementary Table S7. Repeated measures two-way ANOVA tests were performed to assess the effects of drug administration on complete blood cell (CBC) count date by comparing base line measurements to post-drug administration timepoints.

Supplementary Table S8. Repeated measures two-way ANOVA tests were performed to assess the effects of drug administration on blood chemistry data by comparing baseline measurements to post-drug administration timepoints.

Supplementary Table S9. Repeated measures two-way ANOVA tests were performed to assess the effects of drug administration on cytokine data on cytokine data by comparing baseline measurements to post-drug administration timepoints.

Supplementary Fig. S1. Fourteen NHPs were exposed to 4.0 Gy total-body γ-radiation and were administered a single subcutaneous dose of either 37.5 μg/kg (n = 8) or 75 μg/kg (n = 6) dose of BBT-059 24 h postirradiation. Temperature, heart rate, weight, percent weight change, systolic blood pressure, and diastolic blood pressure were monitored for 60 days postirradiation. P values less than 0.05 are denoted with *.

Supplementary Fig. S2. Fourteen NHPs were exposed to 4.0 Gy total-body γ-radiation and were administered a single subcutaneous dose of either 37.5 μg/kg (n = 8) or 75 μg/kg (n = 6) dose of BBT-059 24 h postirradiation. White blood cells (WBCs), red blood cells (RBCs), hemoglobin (HGB), hematocrit (HCT), platelet and neutrophil counts were monitored for 60 days postirradiation. *$P < 0.05$.

Supplementary Fig. S3. Fourteen NHPs were exposed to 4.0 Gy total-body γ-radiation and were administered a single subcutaneous dose of either 37.5 μg/kg (n = 8) or 75 μg/kg (n = 6) dose of BBT-059 24 h postirradiation. Lymphocyte, monocyte, eosinophil, and basophil counts were monitored for 60 days post-irradiation. *$P < 0.05$.

Supplementary Fig. S4. Fourteen NHPs were exposed to 4.0 Gy total-body γ-radiation and were administered a single subcutaneous (*sc*) dose of either 37.5 μg/kg (n = 8) or 75 μg/kg (n = 6) dose of BBT-059 24 h postirradiation. Albumin, alkaline phosphatase (ALP), alanine transaminase (ALT), aspartate aminotransferase (AST), blood urea nitrogen (BUN), and calcium concentrations were monitored for 60 days post-irradiation. *$P < 0.05$.

Supplementary Fig. S5. Fourteen NHPs were exposed to 4.0 Gy total-body γ-radiation and were administered a single subcutaneous (sc) dose of either 37.5 μg/kg (n = 8) or 75 μg/kg (n = 6) dose of BBT-059 24 h postirradiation. Chloride, cholesterol, creatine kinase, creatinine, glucose, and phosphorous concentrations were monitored for 60 days post-irradiation. *$P < 0.05$.

Supplementary Fig. S6. Fourteen NHPs were exposed to 4.0 Gy total-body γ-radiation and were administered a single subcutaneous (sc) dose of either 37.5 μg/kg (n = 8) or 75 μg/kg (n = 6) dose of BBT-059 24 h postirradiation. Potassium, sodium, total bilirubin, and total protein concentrations were monitored for 60 days post-irradiation. *$P < 0.05$.

Supplementary Fig. S7. Fourteen NHPs were exposed to 4.0 Gy total-body γ-radiation and were administered a single subcutaneous (sc) dose of either 37.5 μg/kg (n = 8) or 75 μg/kg (n = 6) dose of BBT-059 24 h postirradiation. IL-16, TNF-α, G-CSF, TNF-β, IL-4, and IL-8 concentrations were monitored for 60 days post-irradiation. *$P < 0.05$.

Supplementary Fig. S8. Fourteen NHPs were exposed to 4.0 Gy total-body γ-radiation and were administered a single subcutaneous (sc) dose of either 37.5 μg/kg (n = 8) or 75 μg/kg (n = 6) dose of BBT-059 24 h postirradiation. SCF, PDGF-BB, MCP-1, IL-18, IL-12p40, and SDF-1α concentrations were monitored for 60 days post-irradiation. *$P < 0.05$.

Supplementary Fig. S9. Fourteen NHPs were exposed to 4.0 Gy total-body γ-radiation and were administered a

single subcutaneous (sc) dose of either 37.5 μg/kg (n = 8) or 75 μg/kg (n = 6) dose of BBT-059 24 h postirradiation. IL-13, LIF, M-CSF, TRAIL, HGF, and IL-9 concentrations were monitored for 60 days post-irradiation. *$P < 0.05$.

ACKNOWLEDGMENTS

The authors would like to thank the staff of the Southern Research Institute for animal care, and the staff of the Radiation Science Department, AFRRI, for dosimetry and radiation exposure to the animals. We also thank Dr. Carmen Rios and Dr. Andrea Dicarlo-Cohen for scientific discussions. The authors would like to acknowledge the Metabolomics Shared Resource in Georgetown University (Washington, DC) partially supported by NIH/NCI/CCSG grant P30-CA051008. The authors gratefully acknowledge the research support from the National Institute of Allergy and Infectious Diseases (AAI12044-001-07000 - Work plan G) as Interagency-Agreements, and the Uniformed Services University of the Health Sciences/Armed Forces Radiobiology Research Institute (grant no. AFR-10978 and 12080) to VKS. The opinions or assertions contained herein are the private views of the authors and are not necessarily those of the Uniformed Services University of the Health Sciences, or the Department of Defense. The mention of specific therapeutic agents does not constitute endorsement by the U.S. Department of Defense, and trade names are used only for the purpose of clarification.

Received: September 26, 2024; accepted: December 11, 2024; published online: December 31, 2024

REFERENCES

1. Strom JS. Health impacts from acute radiation exposure. Office of Security Affairs U.S. Department of Energy under Contract DE-AC06-76RLO 1830. Richland, Washington: Pacific Northwest National Laboratory; 2003.
2. Allio T. Product development under FDA's Animal Rule: Understanding FDA's expectations and potential implication for traditional development programs. Ther Innov Regul Sci 2016; 50: 660–70.
3. U.S. Food and Drug Administration. Guidance document: Product development under the Animal Rule. 2015. Available at: http://www.fda.gov/downloads/drugs/guidancecomplianceregulatoryinformation/guidances/ucm399217.pdf [Last accessed 2022].
4. Dorr H, Meineke V. Acute radiation syndrome caused by accidental radiation exposure - therapeutic principles. BMC Med 2011; 9:126.
5. McCann DGC. Radiation poisoning: Current concepts in the acute radiation syndrome. Am J Clin Med 2006; 3:13–21.
6. Farese AM, MacVittie TJ. Filgrastim for the treatment of hematopoietic acute radiation syndrome. Drugs Today (Barc) 2015; 51: 537–48.
7. Singh VK, Seed TM. An update on sargramostim for treatment of acute radiation syndrome. Drugs Today (Barc) 2018;54:679–93.
8. Singh VK, Seed TM. Radiation countermeasures for hematopoietic acute radiation syndrome: growth factors, cytokines and beyond. Int J Radiat Biol 2021; 97:1526–47.
9. Hankey KG, Farese AM, Blaauw EC, Gibbs AM, Smith CP, Katz BP, et al. Pegfilgrastim improves survival of lethally irradiated nonhuman primates. Radiat Res 2015; 183:643–55.
10. Clayton NP, Khan-Malek RC, Dangler CA, Zhang D, Ascah A, Gains M, et al. Sargramostim (rhu GM-CSF) improves survival of non-human primates with severe bone marrow suppression after acute, high-dose, whole-body irradiation. Radiat Res 2021; 195: 191–9.
11. Zhong Y, Pouliot M, Downey AM, Mockbee C, Roychowdhury D, Wierzbicki W, et al. Efficacy of delayed administration of sargramostim up to 120 hours post exposure in a nonhuman primate total body radiation model. Int J Radiat Biol 2021; 97:S100–S16.
12. Singh VK, Seed TM. An update on romiplostim for treatment of acute radiation syndrome. Drugs Today (Barc) 2022; 58:133–45.
13. Farese AM, Cohen MV, Katz BP, Smith CP, Gibbs A, Cohen DM, et al. Filgrastim improves survival in lethally irradiated nonhuman primates. Radiat Res 2013; 179:89–100.
14. Lazarus HM, McManus J, Gale RP. Sargramostim in acute radiation syndrome. Expert Opin Biol Ther 2022; 22:1345–52.
15. Wong K, Chang PY, Fielden M, Downey AM, Bunin D, Bakke J, et al. Pharmacodynamics of romiplostim alone and in combination with pegfilgrastim on acute radiation-induced thrombocytopenia and neutropenia in non-human primates. Int J Radiat Biol 2020; 96:155–66.
16. Bunin DI, Javitz HS, Gahagen J, Bakke J, Lane JH, Andrews DA, et al. Survival and hematologic benefits of romiplostim after acute radiation exposure supported FDA approval under the animal rule. Int J Radiat Oncol Biol Phys 2023; 17:705–17.
17. Fresenius Kabi. STIMUFEND (pegfilgrastim-fpgk) is biosimilar* to NEULASTA (pegfilgrastim). 2023. Available at: [Last accessed 2023].
18. Coherus BioSciences Inc. UDENYCA (pegfilgrastim-cbqv) is biosimilar* to NEULASTA (pegfilgrastim). 2022. Available at: https://www.accessdata.fda.gov/drugsatfda_docs/label/2022/761039s014lbl.pdf [Last accessed 2023].
19. U.S. Food and Drug Administration. Radiological and nuclear emergency preparedness information from FDA. 2024. Available at: https://www.fda.gov/emergency-preparedness-and-response/mcm-issues/radiological-and-nuclear-emergency-preparedness-information-fda [Last accessed 2024].
20. Singh VK, Garcia M, Seed TM. A review of radiation countermeasures focusing on injury-specific medicinals and regulatory approval status: part II. Countermeasures for limited indications, internalized radionuclides, emesis, late effects, and agents demonstrating efficacy in large animals with or without FDA IND status. Int J Radiat Biol 2017; 93:870–84.
21. Singh VK, Hanlon BK, Santiago PT, Seed TM. A review of radiation countermeasures focusing on injury-specific medicinals and regulatory approval status: part III. Countermeasures under early stages of development along with 'standard of care' medicinal and procedures not requiring regulatory approval for use. Int J Radiat Biol 2017; 93:885–906.
22. Singh VK, Seed TM. A review of radiation countermeasures focusing on injury-specific medicinals and regulatory approval status: part I. Radiation sub-syndromes, animal models and FDA-approved countermeasures. Int J Radiat Biol 2017; 93:851–69.
23. Singh VK, Seed TM. Development of gamma-tocotrienol as a radiation medical countermeasure for the acute radiation syndrome: Current status and future perspectives. Expert Opin Investig Drugs 2023; 32:25–35.
24. Singh VK, Seed TM. BIO 300: A promising radiation countermeasure under advanced development for acute radiation syndrome and the delayed effects of acute radiation exposure. Expert Opin Investig Drugs 2020; 29:429–41.
25. Metcalfe RD, Putoczki TL, Griffin MDW. Structural understanding of interleukin 6 family cytokine signaling and targeted therapies: Focus on interleukin 11. Front Immunol 2020; 11:1424.
26. Singh VK, Seed TM. The safety and efficacy of interleukin 11 for radiation injury. Expert Opin Drug Saf 2023; 22:105–9.
27. Dams-Kozlowska H, Gryska K, Kwiatkowska-Borowczyk E, Izycki D, Rose-John S, Mackiewicz A. A designer hyper interleukin 11 (H11) is a biologically active cytokine. BMC Biotechnol 2012; 12:8.

28. Kaye JA. The clinical development of recombinant human interleukin 11 (NEUMEGA rhIL-11 growth factor). Stem Cells 1996; 14 Suppl 1:256–60.
29. Reynolds CH. Clinical efficacy of rhIL-11. Oncology (Williston Park) 2000; 14:32–40.
30. Burnett AF, Biju PG, Lui H, Hauer-Jensen M. Oral interleukin 11 as a countermeasure to lethal total-body irradiation in a murine model. Radiat Res 2013; 180:595–602.
31. Potten CS. Protection of the small intestinal clonogenic stem cells from radiation-induced damage by pretreatment with interleukin 11 also increases murine survival time. Stem Cells 1996; 14:452–9.
32. Hao J, Sun L, Huang H, Xiong G, Liu X, Qiu L, et al. Effects of recombinant human interleukin 11 on thrombocytopenia and neutropenia in irradiated rhesus monkeys. Radiat Res 2004; 162:157–63.
33. Kumar VP, Biswas S, Sharma NK, Stone S, Fam CM, Cox GN, et al. PEGylated IL-11 (BBT-059): A novel radiation countermeasure for hematopoietic acute radiation syndrome. Health Phys 2018; 115:65–76.
34. Plett PA, Chua HL, Sampson CH, Katz BP, Fam CM, Anderson LJ, et al. PEGylated G-CSF (BBT-015), GM-CSF (BBT-007), and IL-11 (BBT-059) analogs enhance survival and hematopoietic cell recovery in a mouse model of the hematopoietic syndrome of the acute radiation syndrome. Health Phys 2014; 106:7–20.
35. Bolder BioTechnology. Pipeline. 2017. Available at: http://www.bolderbio.com/pipeline/ [Last accessed 2023].
36. Singh VK, Olabisi AO. Nonhuman primates as models for the discovery and development of radiation countermeasures. Expert Opin Drug Discov 2017; 12:695–709.
37. Carpenter A, Li Y, Wise SY, Fatanmi OO, Petrus SA, Fam CM, et al. Pharmacokinetic and metabolomic studies with a promising radiation countermeasure, BBT-059 (PEGylated interleukin-11), in rhesus nonhuman primates. Radiat Res 2024; 202:26–37.
38. Tuntland T, Ethell B, Kosaka T, Blasco F, Zang RX, Jain M, et al. Implementation of pharmacokinetic and pharmacodynamic strategies in early research phases of drug discovery and development at Novartis Institute of Biomedical Research. Front Pharmacol 2014; 5:174.
39. Crook A, De Lima Leite A, Payne T, Bhinderwala F, Woods J, Singh VK, et al. Radiation exposure induces cross-species temporal metabolic changes that are mitigated in mice by amifostine. Sci Rep 2021; 11:14004.
40. Cheema AK, Li Y, Girgis M, Jayatilake M, Fatanmi OO, Wise SY, et al. Alterations in Tissue Metabolite Profiles with Amifostine-Prophylaxed Mice Exposed to Gamma Radiation. Metabolites 2020; 10.
41. Cheema AK, Li Y, Girgis M, Jayatilake M, Simas M, Wise SY, et al. Metabolomic studies in tissues of mice treated with amifostine and exposed to gamma-radiation. Sci Rep 2019; 9:15701.
42. Singh VK, Seed TM. The efficacy and safety of amifostine for the acute radiation syndrome. Expert Opin Drug Saf 2019; 18:1077–90.
43. Li Y, Girgis M, Jayatilake M, Serebrenik AA, Cheema AK, Kaytor MD, et al. Pharmacokinetic and metabolomic studies with a BIO 300 oral powder formulation in nonhuman primates. Sci Rep 2022; 12:13475.
44. Cheema AK, Mehta KY, Santiago PT, Fatanmi OO, Kaytor MD, Singh VK. Pharmacokinetic and metabolomic studies with BIO 300, a nanosuspension of genistein, in a nonhuman primate model. Int J Mol Sci 2019; 20:1231.
45. Li Y, Girgis M, Wise SY, Fatanmi OO, Seed TM, Maniar M, et al. Analysis of the metabolomic profile in serum of irradiated nonhuman primates treated with Ex-Rad, a radiation countermeasure. Sci Rep 2021; 11:11449.
46. Pannkuk EL, Laiakis EC, Fornace AJ, Jr., Fatanmi OO, Singh VK. A metabolomic serum signature from nonhuman primates treated with a radiation countermeasure, gamma-tocotrienol, and exposed to ionizing radiation. Health Phys 2018; 115:3–11.
47. Cheema AK, Mehta KY, Fatanmi OO, Wise SY, Hinzman CP, Wolff J, et al. A Metabolomic and lipidomic serum signature from nonhuman primates administered with a promising radiation countermeasure, gamma-tocotrienol. Int J Mol Sci 2018; 19:79.
48. U.S. Food and Drug Administration. Guidance for Industry: Estimating the maximum safe starting dose in initial clinical trials for therapeutics in adult healthy volunteers. 2005. Available at: https://www.fda.gov/regulatory-information/search-fda-guidance-documents/estimating-maximum-safe-starting-dose-initial-clinical-trials-therapeutics-adult-healthy-volunteers [Last accessed 2023].
49. Singh VK, Kulkarni S, Fatanmi OO, Wise SY, Newman VL, Romaine PL, et al. Radioprotective efficacy of gamma-tocotrienol in nonhuman primates. Radiat Res 2016; 185:285–98.
50. Phipps AJ, Bergmann JN, Albrecht MT, Singh VK, Homer MJ. Model for evaluating antimicrobial therapy to prevent life-threatening bacterial infections following exposure to a medically significant radiation dose. Antimicrob Agents Chemother 2022; 66:e0054622.
51. Vellichirammal NN, Sethi S, Pandey S, Singh J, Wise SY, Carpenter AD, et al. Lung transcriptome of nonhuman primates exposed to total- and partial-body irradiation. Mol Ther Nucleic Acids 2022; 29:584–98.
52. Nagy V. Accuracy considerations in EPR dosimetry. Appl Radiat Isot 2000; 52:1039–50.
53. International Standardization Organization and ASTM International. Standard Practice for Use of an Alanine-EPR Dosimetry System. Geneva, Switzerland: ASTM International, ISO and West Conshohocken (US:PA); 2013. p. 7.
54. Cheema AK, Li Y, Moulton J, Girgis M, Wise SY, Carpenter A, et al. Identification of novel biomarkers for acute radiation injury using multiomics approach and nonhuman primate model. Int J Radiat Oncol Biol Phys 2022; 114:310–20.
55. Singh VK, Fatanmi OO, Wise SY, Carpenter AD, Olsen CH. Determination of lethality curve for cobalt-60 gamma-radiation source in rhesus macaques using subject-based supportive care. Radiat Res 2022; 198:599–614.
56. Kulkarni S, Singh PK, Ghosh SP, Posarac A, Singh VK. Granulocyte colony-stimulating factor antibody abrogates radioprotective efficacy of gamma-tocotrienol, a promising radiation countermeasure. Cytokine 2013; 62:278–85.
57. Carpenter AD, Fatanmi OO, Wise SY, Petrus SA, Tyburski JB, Cheema AK, et al. Metabolomic changes in plasma of preterminal stage of rhesus nonhuman primates exposed to lethal dose of radiation. Metabolites 2024; 14:18.
58. Carpenter AD, Li Y, Fatanmi OO, Wise SY, Petrus SA, Janocha BL, et al. Metabolomic profiles in tissues of nonhuman primates exposed to total- or partial-body radiation. Radiat Res 2024; 201:371–83.
59. Libiseller G, Dvorzak M, Kleb U, Gander E, Eisenberg T, Madeo F, et al. IPO: a tool for automated optimization of XCMS parameters. BMC Bioinformatics 2015; 16:118.
60. Smith CA, Want EJ, O'Maille G, Abagyan R, Siuzdak G. XCMS: processing mass spectrometry data for metabolite profiling using nonlinear peak alignment, matching, and identification. Anal Chem 2006; 78:779–87.
61. Dunn WB, Broadhurst D, Begley P, Zelena E, Francis-McIntyre S, Anderson N, et al. Procedures for large-scale metabolic profiling of serum and plasma using gas chromatography and liquid chromatography coupled to mass spectrometry. Nat Protoc 2011; 6:1060–83.
62. Yan X, Liu, X.-P., Guo, Z.-X., Liu, T.-Z. & Li, S. dentification of hub genes associated with progression and prognosis in patients with bladder cancer. Front Genet 2019; 20:408.
63. Sharma NK, Holmes-Hampton GP, Kumar VP, Biswas S, Wuddie K, Stone S, et al. Delayed effects of acute whole body lethal radiation exposure in mice pre-treated with BBT-059. Sci Rep 2020; 10:6825.

64. Li Y, Wu Q, Jin Y, Yang Q. Antiviral activity of interleukin-11 as a response to porcine epidemic diarrhea virus infection. Vet Res 2019; 50:111.

65. Laiakis EC, Wang YW, Young EF, Harken AD, Xu Y, Smilenov L, et al. Metabolic Dysregulation after Neutron Exposures Expected from an Improvised Nuclear Device. Radiat Res 2017; 188:21–34.

66. Cheema AK, Mehta KY, Rajagopal MU, Wise SY, Fatanmi OO, Singh VK. Metabolomic studies of tissue injury in nonhuman primates exposed to gamma-radiation. Int J Mol Sci 2019; 20:3360.

67. Menon SS, Uppal M, Randhawa S, Cheema MS, Aghdam N, Usala RL, et al. Radiation metabolomics: Current status and future directions. Front Oncol 2016; 6:20.

68. Chickos JS, Way BA, Wilson J, Shaharuzzaman M, Laird J, Landt M. Analysis of 3-hydroxydodecanedioic acid for studies of fatty acid metabolic disorders: preparation of stable isotope standards. J Clin Lab Anal 2002; 16:115–20.

69. Singh VK, Seed TM, Cheema AK. Metabolomics-based predictive biomarkers of radiation injury and countermeasure efficacy: Current status and future perspectives. Expert Rev Mol Diagn 2021; 21:641–54.

70. Cheema AK, Hinzman CP, Mehta KY, Hanlon BK, Garcia M, Fatanmi OO, et al. Plasma derived exosomal biomarkers of exposure to ionizing radiation in nonhuman primates. Int J Mol Sci 2018; 19:3427.

71. Pannkuk EL, Laiakis EC, Garcia M, Fornace AJ, Jr., Singh VK. Nonhuman primates with acute radiation syndrome: Results from a global serum metabolomics study after 7.2 Gy total-body irradiation. Radiat Res 2018; 190:576–83.

72. Pannkuk EL, Laiakis EC, Singh VK, Fornace AJ. Lipidomic signatures of nonhuman primates with radiation-induced hematopoietic syndrome. Sci Rep 2017; 7:9777.

73. Tichy A, Carpenter AD, Li Y, Rydlova G, Rehulka P, Markova M, et al. Radiation signature in plasma metabolome of total-body irradiated nonhuman primates and clinical patients. Int J Mol Sci 2024; 25:9208.

74. Widjaja AA, Chothani S, Viswanathan S, Goh JWT, Lim WW, Cook SA. IL11 Stimulates IL33 Expression and Proinflammatory Fibroblast Activation across Tissues. Int J Mol Sci 2022; 23.

75. National Research Council of the National Academy of Sciences. Guide for the care and use of laboratory animals. 8th ed. Washington, DC: National Academies Press; 2011.